BIOLOGY OF REPRODUCTION (2012) **86**(4):115, 1–10
Published online before print 11 January 2012.
DOI 10.1095/biolreprod.111.096925

The Molecular Role of Connexin 43 in Human Trophoblast Cell Fusion[1]

Caroline E. Dunk,[2,3] Alexandra Gellhaus,[4] Sascha Drewlo,[3] Dora Baczyk,[3] Andy J.G. Pötgens,[5] Elke Winterhager,[4] John C.P. Kingdom,[6] and Steven J. Lye[3,6]

[3]*Research Centre for Women's and Infants' Health, Samuel Lunenfeld Research Institute, Mount Sinai Hospital, University of Toronto, Toronto, Ontario, Canada*
[4]*Institute of Molecular Biology, University of Duisburg-Essen, Essen, Germany*
[5]*Institute of Anatomy, University Hospital RWTH, Aachen, Germany*
[6]*Department of Obstetrics and Gynecology, Mount Sinai Hospital, University of Toronto, Toronto, Ontario, Canada*

ABSTRACT

Connexin expression and gap junctional intercellular communication (GJIC) mediated by connexin 43 (Cx43)/gap junction A1 (GJA1) are required for cytotrophoblast fusion into the syncytium, the outer functional layer of the human placenta. Cx43 also impacts intracellular signaling through protein-protein interactions. The transcription factor GCM1 and its downstream target ERVW-1/SYNCYTIN-1 are key players in trophoblast fusion and exert their actions through the ERVW-1 receptor SLC1A5/ASCT-2/RDR/ATB(0). To investigate the molecular role of the Cx43 protein and its interaction with this fusogenic pathway, we utilized stable Cx43-transfected cell lines established from the choriocarcinoma cell line Jeg3: wild-type Jeg3, alphahCG/Cx43 (constitutive Cx43 expression), JpUHD/Cx43 (doxycyclin-inducible Cx43 expression), or JpUHD/trCx43 (doxycyclin-inducible Cx43 carboxyterminal deleted). We hypothesized that truncation of Cx43 at its C-terminus would inhibit trophoblast fusion and protein interaction with either ERVW-1 or SLC1A5. In the alphahCG/Cx43 and JpUHD/Cx43 lines, stimulation with cAMP caused 1) increase in *GJA1* mRNA levels, 2) increase in percentage of fused cells, and 3) downregulation of SLC1A5 expression. Cell fusion was inhibited by GJIC blockade using carbenoxylone. Neither Jeg3, which express low levels of Cx43, nor the JpUHD/trCx43 cell line demonstrated cell fusion or downregulation of SLC1A5. However, *GCM1* and *ERVW-1* mRNAs were upregulated by cAMP treatment in both Jeg3 and all Cx43 cell lines. Silencing of *GCM1* prevented the induction of *GJA1* mRNA by forskolin in BeWo choriocarcinoma cells, demonstrating that GCM1 is upstream of Cx43. All cell lines and first-trimester villous explants also demonstrated coimmunoprecipitation of SLC1A5 and phosphorylated Cx43. Importantly, SLC1A5 and Cx43 gap junction plaques colocalized in situ to areas of fusing cytotrophoblast, as demonstrated by the loss of E-cadherin staining in the plasma membrane in first-trimester placenta. We conclude that Cx43-mediated GJIC and SLC1A5 interaction play important functional roles in trophoblast cell fusion.

connexin 43 (Cx43), ERVW-1/SYNCYTIN-1, SLC1A5/ASCT-2/RDR/ATB(0), syncytiotrophoblast, trophoblast fusion

INTRODUCTION

The syncytiotrophoblast layer of the human placenta is the functional barrier and the site of numerous exchanges between the maternal and fetal circulations. It is initially formed at the time of implantation by the direct fusion of mononuclear cytotrophoblast and subsequently maintained over the course of the pregnancy by continuous fusion of cytotrophoblast with the overlying syncytiotrophoblast [1]. This donation of cytotrophoblastic cell contents is absolutely required for syncytial health and function, because nuclear division does not occur within the syncytiotrophoblast [2]. Trophoblast cell fusion can be reproduced in vitro and is dependent on gap junctional intercellular communication (GJIC) specifically mediated by connexin 43 (Cx43)/gap junction A1 (GJA1) [3–5].

Gap junction channels formed from hexamers of connexin proteins are responsible for direct intercellular communication between adjacent cells. The direct exchange of small molecules, ions, and second messengers, such as cAMP, cGMP, inositol phosphate, and Ca^{2+}, between cells is thought to enable the channels to control and coordinate cell growth [6, 7]. This is of interest, because cytotrophoblast must exit the cell cycle to fuse into the syncytium [8]. How gap junctions control the cell cycle is not fully understood, because the Cx43 protein itself, independent from gap junction channel formation, is able to affect growth control as well as further cellular functions, such as adhesion and migration [9–12]. Indeed, we have previously shown that stable transfection and expression of Cx43 in the Jeg3 choriocarcinoma cell line results in an inhibition of cell growth as compared to the wild-type cells, whereas the truncated Cx43 (trCx43) protein lacking the cytoplasmic tail of Cx43 has no effect [13]. It was further demonstrated that this growth suppression was dependent on the interaction of the Cx43 cytoplasmic tail with a CCN family negative growth-regulating protein nephroblastoma overexpressed gene (NOV; CCN3) and a shift in its localization from the nucleus to the cytoplasmic membrane [13]. However, subsequent studies demonstrated that NOV is restricted to the invasive extravillous trophoblast of the human placenta [14], suggesting that an alternate pathway may mediate Cx43-driven villous cytotrophoblast differentiation to the syncytiotrophoblast. The carboxyterminus of Cx43 contains numerous phosphorylation sites for protein kinases [15]. Of particular interest, tight junction protein (TJP) 1 binds in the last 20 amino acids of the carboxyterminus [16] and is involved in the regulation of trophoblast fusion and Cx43 protein expression [17].

[1]Supported by the Canadian Institutes of Health Research (MOP 82811 to S.J.L. and MOP 64302 to J.C.P.K.) and the Deutsche Forschungsgemeinschaft (DFG; Wi 774/21-2 and Wi 774/22-1 to E.W. and A.G.).
[2]Correspondence: Caroline Dunk, Research Centre for Women's and Infants' Health, Rm 6-1025, Samuel Lunenfeld Research Institute, Mount Sinai Hospital, 25 Orde St., Toronto, ON M5T 3H7, Canada. E-mail: dunk@lunenfeld.ca

Received: 12 October 2011.
First decision: 16 November 2011.
Accepted: 21 December 2011.

eISSN: 1529-7268 http://www.biolreprod.org
ISSN: 0006-3363

In the human placenta, the ''precursor'' cytotrophoblast proliferates to form daughter cytotrophoblasts that are destined for syncytial fusion [18, 19]. These postmitotic daughter cytotrophoblast cells express the transcription factor glial cell missing 1 (GCM1), a key mediator of trophoblast turnover and syncytial formation [20, 21]. It has been proposed that the fusogenic effects of GCM1 are mediated by upregulation of the human endogenous retrovirus W (HERV-W) retroviral envelope protein endogenous retrovirus W-1 (ERVW-1)/SYNCYTIN-1 in cytotrophoblast [22, 23]. ERVW-1 in turn mediates its effects by interacting with its receptor the solute carrier family 1 member 5 (SLC1A5)/neutral amino acid transporter (ASCT-2)/type D mammalian retrovirus receptor (RDR)/amino acid transporter system B0 (ATB[0]), which is expressed by the syncytiotrophoblast [22, 24, 25].

In the present study, we investigate the molecular interactions between Cx43, GJIC, and the GCM1-ERVW-1-SLC1A5 pathway during trophoblast cell fusion in vitro using Jeg3 cell lines stably expressing both constitutive or inducible Cx43 and using first-trimester placental villous tissue. To discriminate whether the Cx43 protein itself affects cell-cell fusion as a result of the intercellular exchange of molecules through the channel or by intracellular signaling via the carboxyterminus, we used a mutated form of Cx43 (trCx43) that lacks the carboxyterminus. We have previously demonstrated that trCx43 forms a functional gap junction channel and mediates GJIC, as shown by immunofluorescence and calcein dye transfer assay [13]. All cell lines were treated with cAMP over a 72-h time course, and levels of cell fusion, GCM1, ERVW-1, SLC1A5, and Cx43 expression were assessed. We also investigated the interaction of Cx43 and SLC1A5 in the cell lines and in vivo in first-trimester human placenta.

MATERIALS AND METHODS

Cell Lines

The human choriocarcinoma cell line Jeg3 (ATCC HTB-36) was purchased from the American Type Culture Collection. Jeg3 cells were grown in Minimum Essential Medium (MEM; Invitrogen) supplemented with 10% fetal calf serum (FCS; certified tetracycline-free; Fisher Thermo Scientific), G418, and amphotericin B at standard culture conditions of 37°C and 5% CO_2. Stable Jeg3 clones expressing constitutive α-human chorionic gonadotropin (hCG)-Cx43 (generated by ligation of the 900-bp human αhCG promoter fragment into pBluescript SK(+/–) via *Hin*dIII together with a 1.4-kb rat Cx43 fragment by *Eco*RV/*Not*I restriction digestion), doxycycline-inducible full-length JpUHD/Cx43, and doxycycline-inducible JpUHD/trCx43 (missing amino acids 259–382), were generated as previously described [13]. Plasmid expression was maintained by selection for puromycin resistance 0.5 μg/ml puromycin (Sigma), and Cx43 and Cx40 expression was induced in the JpUHD lines by the addition of 1 μg/ml of Doxycycline HCL (Sigma) to the culture medium for 48 h before initiation of the experiment.

Tissue Collection and Culture

First-trimester placentas were collected following termination of pregnancy with informed patient consent. All tissue collections were approved by the Morgantaler Clinic (Toronto, ON, Canada) and the Research Ethics board of Mount Sinai Hospital. Floating villous placental explants were examined under a dissecting microscope and selected by the absence of extravillous trophoblast columns. Explants were placed in tissue culture plates containing Dulbecco modified Eagle medium/Ham F12 supplemented with 1% Insulin-Transferrin-Selenium-A (Invitrogen) and cultured with or without 1 μM 8-bromo-cAMP (Calbiochem) at 37°C with 5% CO_2 and 8% O_2 for 24 h. Explants were collected for protein extraction and immunoprecipitation as described below.

Two-Color Cell Fusion Assay

The two-color cell fusion assay was performed as previously described by Borges et al. [26]. Briefly, confluent cells from each cell line were trypsinized, centrifuged ($80 \times g$ for 5 min), and counted before division of equal numbers of cells into two tubes. Cells were then centrifuged again ($80 \times g$ for 5 min) and resuspended in serum-free medium to a final cell number of 1×10^6 cells/ml and labeled with either 5 μM Cytotracker CMTMDR (red) in one tube or 5 μM Cytotracker CMFDA (green; both from Molecular Probes, Invitrogen) in the second tube. Labeled cells were washed in MEM with 10% FCS, counted, and diluted to 1×10^5 cells/ml before seeding in six-well plates at a density of 1×10^5 green cells/well and 1×10^5 orange cells/well. Cells were allowed to adhere for 6 h and then stimulated with 1 μM 8-bromo-cAMP with or without 125 μM carbenoxylone (CBX; Sigma) or 125 μM glycyrrhizic acid (GZA; Sigma), its inactive analog. Cell-cell fusion events were determined using a 1X51 inverted fluorescent microscope (Olympus) to capture five random phase-contrast images with matching fluorescent images per well over a 3-day time course at 24, 48, and 72 h. The fusion index was calculated as a percentage of nuclei in double fluorescent cytoplasm/total nuclei per field of view. Data was assessed by two independent investigators (Sabrina Pavri and Iskra Peltekova) blinded to cell line and treatment group. All experiments were performed in triplicate wells and as four independent experiments.

Northern Blot Analysis

Total RNA was isolated from confluent cell monolayers using Qiagen RNeasy Kit (Qiagen). RNA was separated on 1% (wt/vol) agarose (Invitrogen) gel containing 3.7% (vol/vol) formaldehyde (Fisher Thermo Scientific) in MOPS (3-[*N*-morpholino]-propanesulfonic acid; Sigma), transferred in 0.1 M sodium phosphate (Sigma) on to a nylon membrane (GeneScreen; NEN Life Science Products, Inc.), and cross-linked by ultraviolet irradiation. Hybridization at 55°C and labeling of the specific probes with [α-^{32}P]dCTP by using the random hexamer-primed labeling system (GE Healthcare) were performed as described previously [27]. The following probes were used: human *GCM1* [20], human *ERVW-1* [26], and rat heart *GJA1* cDNA fragment [27]. As a control, the blots were rehybridized with a 18S rRNA-specific probe [28]. Subsequently, the membrane was washed to a final stringency of 30 mM sodium phosphate/0.1% (wt/vol) sodium dodecyl sulfate. Probed membranes were exposed to x-ray film (Kodak XAR; Eastman Kodak) with an intensifying screen at −80°C and analyzed by densitometry.

BeWo Cell Culture and Silencing of GCM1

The human choriocarcinoma cell line BeWo (passages 10–20) was maintained in F12K medium (ATCC) supplemented with 10% fetal bovine serum, 100 units/ml of penicillin, 100 units/ml of streptomycin, and 2.5 μg/ml of fungizone (Invitrogen) in atmospheric O_2/5% CO_2 at 37°C. Two double-stranded siRNA oligonucleotides (21mer) named 201 and 815 against the human *GCM1* sequence (Qiagen) were used as described previously [21]. Confluent BeWo cells were transfected with 50 nM of a 1:1 cocktail of 201 and 815 *GCM1* siRNA or nonsilencing control siRNA for 12 h before stimulation with 50 μM forskolin and subsequent 48-h incubation. Experiments with fluorescent-labeled siRNA established 80%–90% transfection efficiency (data not shown). Toxicity of siRNA treatment was monitored with Human Interferon Alpha ELISA kit (PBL Biomedical Laboratories).

Real-Time RT-PCR Analysis

The RNA samples from each cell line were column purified using RNeasy Mini Kit (Qiagen) and treated with 2.5 μl of DNase I (2.73 Kunitz unit/μl; Qiagen) to remove genomic DNA contamination. Real-time RT-PCR was performed to detect the mRNA expression of *SLC1A5* or *GJA1* in control and cAMP/forskolin-treated cells. A total of 1 μg of RNA was primed with random hexamers to synthesize single-strand cDNAs in a total reaction volume of 50 μl using the TaqMan Reverse Transcription Kit (Applied Biosystems). The thermal cycling parameters of the reverse transcription were modified according to the Applied Biosystems manual. Hexamer incubation at 25°C for 10 min and RT at 42°C for 30 min were followed by reverse transcriptase inactivation at 95°C for 5 min. Then, 20 ng of cDNA from the previous step were subjected to real-time RT-PCR using specific sets of primers for the gene of interest, *SLC1A5*, and three housekeeping genes (*SLC1A5*: forward, 5′-CCGCTTCTTCAACTCCTTCAA-3′; reverse, 5′-ACCCACATCCTCC ATCTCCA-3′ [29]; *GJA1*: forward, 5′-GGGGGATCCATGGGTGACTCGA GC-3′; reverse, 5′-GGGAAGCTTCTAGATCTCCAGGTCAT-3′; *GCM1* [21], *HPRT*: forward, 5′-TGACA CTGGCAAAACAATGCA-3′; reverse, 5′-GGTCCTTTTCACCAGCAAGCT-3′; *YWHAZ*: forward, 5′-ACTTTTGGTA CATTGTGGCTTCAA-3′; reverse, 5′-CCGCCAGGACAAACCAGTAT-3′; and *RN18S*: forward, 5′GCCAAAGCATTTGCCAAGAA-3′; reverse, 5′-GGCATCCTTTATGGTCGGATC-3′) in a total reaction volume of 25 μl (Applied Biosystems). Real-time RT-PCR was performed in an optical 96-well plate with an ABI PRISM 7900 HT Sequence Detection System (Applied

Biosystems) using SYBR Green detection chemistry (Bio-Rad). The run protocol was as follows: initial denaturation stage at 95°C for 10 min, followed by 40 cycles of amplification at 95°C for 15 sec and 60°C for 1 min. After PCR, a dissociation curve was constructed by increasing temperature from 65°C to 95°C for detection of PCR product specificity. In addition, a no-template control (H_2O control) was analyzed for possible contamination in the master mix. A cycle threshold (Ct) value was recorded for each sample. PCR reactions were set up in triplicates, and the mean of the three Ct values was calculated. An arithmetic formula from the comparative Ct method (see ABI User Bulletin 2, http://www3.appliedbiosystems.com/cms/groups/mcb_supportdocuments/generaldocuments/cms_040980.pdf) was applied to the raw Ct values to extract relative gene expression data as compared to the 24-h control sample in each cell line. The *SLC1A5*, *GJA1,* or *GCM1* mRNA level from each sample was normalized to the geometric mean of the *HPRT, YWHAZ,* and ribosomal *RN18S* mRNA. Validation experiments were performed to ensure the PCR efficiencies between all primer sets were approximately equal.

Western Blot Analysis

Equal amounts of total proteins from each cell line treated with either control serum-free medium or 1 μM 8-bromo-cAMP over a 48-h time course were analyzed by Western blot analysis as previously described [30]. Briefly, 20 μg of proteins were added to 5 μl of 4× reducing loading buffer (1 mM β-mercaptoethanol; Invitrogen) and boiled for 5 min. Proteins were run on a 10% SDS-PAGE gel and transferred to a polyvinylidene fluoride (PVDF) membrane (Millipore) overnight at 4°C. Membranes were blocked with 10% nonfat milk and 0.1% bovine serum albumin in Tris-buffered saline with Tween (TBS-T; 10 mM Tris [pH 7.5], 100 mM NaCl, and 0.1% Tween 20) for 1 h at room temperature, followed by three 5-min TBS-T washes. Membranes were incubated with either primary rabbit polyclonal anti-SLC1A5 antibody (1:5000; Fisher Thermo Scientific) or rabbit polyclonal anti-Cx43 antibody (1:1000; Invitrogen) in 5% milk overnight at 4°C followed by three 5-min washes and a 1-h incubation with anti-rabbit-mouse horseradish peroxidase (HRP; 1:3000)-linked secondary antibody (GE Healthcare) at room temperature. Antibody reactions were detected using WesternC Chemiluminescence Detection Kit (Bio-Rad) followed by detection of chemiluminescence using a Versa Doc 5 gel documentation machine (Bio-Rad). To ensure equal loading of the gel, membranes were stripped and reprobed using a mouse monoclonal anti-TUBULIN antibody (1:2000; Sigma). Band intensity and area was analyzed using Quantity One 4.6.7 software (Bio-Rad).

In Vitro Coimmunoprecipitation

Total cell and villous explant proteins were extracted on ice in RIPA buffer (100 mM Tris HCL [pH 7.6], 1% NP-40, 1 mM ethylenediaminetetra-acetic acid, 1 mM ethyleneglycoltetra-acetic acid, 1 mM sodium vanadate, and 1 mM sodium fluoride; Sigma) and protease inhibitor cocktail (Roche) from 48-h time point control and cAMP-treated Jeg3, αhCG/Cx43, JpuHD/Cx43, and JpuHD/trCx43 cell lines. Proteins were precleared by the addition of 20 μl of Protein A Sepharose beads (Pharmacia) and a 2-h incubation at 4°C. Supernatants were collected and total protein concentration assessed before the addition of either 1 μg/ml of polyclonal rabbit anti-SLC1A5 antibody or 1 μg/ml of monoclonal mouse anti-Cx43 antibody (Upstate Cell Signaling Solutions) against the alpha1 domain of the Cx43 protein per 250 μl of 1 mg/ml of total protein per sample and further 2-h incubation with rotation at 4°C. Immunoprecipitation was performed by the addition of 25 μl of Protein A Sepharose beads to each tube and a further incubation with rotation at 4°C overnight. Conjugated beads were collected by centrifugation (4000 rpm for 15 min at 4°C) and washed three times for 2 min with RIPA buffer before addition of 25 μl of reducing 2× SDS sample buffer (Invitrogen) and heating at 95°C-100°C for 5 min. Associated proteins were separated on 10% SDS PAGE gel and transferred to a PVDF membrane (Fisher Thermo Scientific) followed by Western blot analysis with either the monoclonal mouse anti-Cx43 antibody or a goat polyclonal anti-SLC1A5 antibody (Santa Cruz Biotechnology, Inc.). Bands were detected using either anti-mouse HRP antibody (1:3000; GE Healthcare) or anti-goat HRP (1:2000; AbD Serotec) and ECL chemiluminescence exposed to x-ray film (Kodak Scientific).

Triple Immunofluorescence

First-trimester placental biopsies were dehydrated in a 5%–20% sucrose gradient (20 min in each) followed by a 20-min incubation in 20% sucrose and 50% OCT (Bayer) and then were cryoembedded in OCT. Triple-fluorescent immunohistochemistry was performed on frozen sections (thickness, 10 μm) that were air-dried and fixed in a 50%–90% ethanol gradient in PBS. Sections were rehydrated through the ethanol gradient (2 min at each step) and washed in PBS. Antigen retrieval was performed using 0.01% Triton X-100 for 10 min at room temperature. Endogenous fluorescence was blocked by a 1-min incubation in 1% Sudan Black (Sigma) in 70% ethanol followed by nonspecific antigen blocking using 10% normal goat serum, 2% donkey serum (Jackson ImmunoResearch), and 2% human serum (in house) for 1 h at room temperature. Rabbit polyclonal anti-Cx43 antibody (1:100), goat polyclonal anti-SLC1A5 antibody (0.5 μg/ml;), and mouse monoclonal E-cadherin antibody (1:400; Abcam) were added in combination and incubated overnight at 4°C. Following two 5-min washes in PBS, goat anti-rabbit biotinylated (1:300; DAKO), donkey anti-goat Alexa Fluor 546 (1:100; Invitrogen), and donkey anti-mouse Alexa Fluor 488 antibodies were added for 1 h at room temperature. Sections were washed and finally incubated with Streptavidin Alexa Fluor 647 (1:1000; Invitrogen) with 4′,6-diamidino-2-phneylindole (DAPI; Vector Laboratories) counterstaining of nuclei. Negative controls were performed using a combination of mouse and rabbit immunoglobulin (Ig) G or goat IgG matching the concentration of primary antibodies or omission of the first secondary antibody to control for cross-reactivity between the first primary and the second secondary antibodies. Slides were mounted in Immu-Mount (Fisher Thermo Scientific) and images captured using a Quorum Wave FX spinning disk confocal system comprising a Leica DMI 6000B microscope with a Yokoqawa Spinning Head and Image EM Hamematsu EMCCD camera and Velocity imaging software (Improvision). DAPI images of fluorescent nuclei were converted to white for presentation purposes.

Statistical Analysis

Statistical analysis of data was performed using GraphPad Prism (GraphPad Software) on normally distributed data using a one way ANOVA with a Dunnett multiple-comparison test. Data are presented as the mean ± SD of at least three independent experiments (error bars represent the SD in the figure legend) performed in triplicate. *P*-values of less than 0.05 as compared with respective controls are considered to be significant.

RESULTS

Deletion of the Cx43 Cytoplasmic Tail Prevents cAMP-Mediated Cell Fusion

Wild-type Jeg3 cells maintained separation of the red and green cytoplasmic dyes under both control (48 h) (Fig. 1A) and cAMP-treated (48 h) (Fig. 1B) conditions. Constitutive expression of Cx43 induced by the *αhCG* promoter resulted in a small increase in cell-cell fusion under control conditions by 48 h (seen by dissolution of the red dye between red cells in Fig. 1C, arrow). In contrast, treatment with cAMP for 48 h induced high levels of cell fusion across the culture, and mixing of the two dyes was clearly observed, as indicated by red nuclei surrounded by green cytoplasm (Fig. 1D, arrow). Doxycyclin induction of Cx43 in the JpUHD/Cx43 line had little effect in the control conditions, and dyes remained separate (48 h) (Fig. 1E). In contrast, 48 h stimulation with cAMP resulted in the formation of syncytial colonies with loss of membranes containing mixed red and green nuclei (Fig. 1F, arrows). Induction of the trCx43 protein in the JpUHD/trCx43 cell line resulted in the continued segregation of the dyes in both control (Fig. 1G) and cAMP-treated (Fig. 1H) after 48 h. In our experiments, a Jeg3 cell line transfected with Cx40 demonstrated only endomitosis when stimulated with cAMP, as was observed by the continued segregation of the dyes even after 96 h of treatment (Supplemental Fig. S1, I and J; all Supplemental Data are available online at www.biolreprod.org).

Quantification of the fusion index of all cell lines over a 72-h time course by two independent investigators comparing the merged two-color images and the matching phase-contrast images (Supplemental Fig. S1) demonstrated that the αhCG/Cx43 line displayed a rapid response to cAMP stimulation, because by 24 h of treatment, 58.98% ± 20.16% of the nuclei were in fused compartments as compared to control cells at 23.47% ± 6.91% ($P < 0.01$, $n = 4$) (Fig. 2A). This percentage did not significantly increase on further stimulation with cAMP at either 48 or 72 h, although at both time points, a significantly

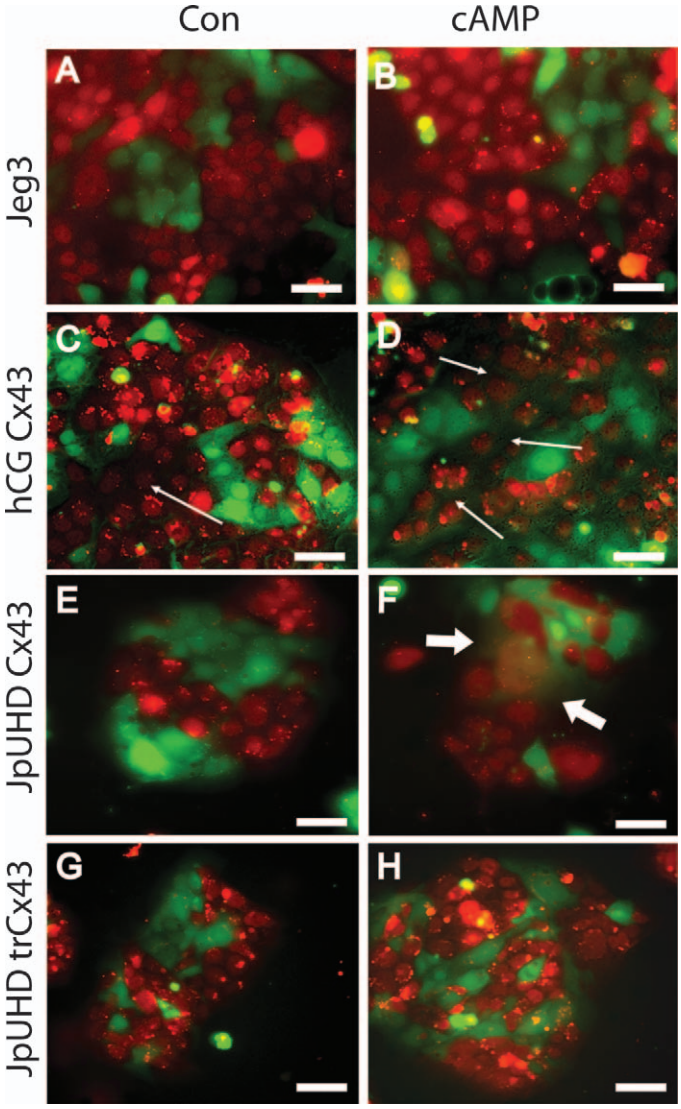

FIG. 1. Cyclic AMP stimulates cell-cell fusion in full length Cx43-expressing cell lines. Two-color cell fusion assay was performed using wild-type Jeg3 (**A** and **B**), αhCG/Cx43 (**C** and **D**), JpUHD/Cx43 (**E** and **F**), and JpUHD/trCx43 (**G** and **H**) cell lines. Cells were stimulated with control serum-free medium (**A**, **C**, **E**, and **F**) or 1 μM 8-bromo-cAMP (**B**, **D**, **F**, and **H**) for 48 h. Cell-cell fusion, indicated by the mixing of the red and green dyes to give either red nuclei surrounded by green cytoplasm or green nuclei surrounded by red cytoplasm, can be observed in the cAMP-treated αhCG/Cx43 (fine arrows, **D**) and JpUHD/Cx43 (bold arrows, **F**) cells. Bar = 25 μm.

higher percentage of fused cells was observed over that in the corresponding control cells. The inducible JpUHD/Cx43 cell line showed a more gradual response to cAMP that reached significance at 72 h of treatment as compared to control cells (48.19% ± 17.25% vs. 19.65% ± 10.79, $P < 0.01$, n = 4). Neither wild-type Jeg3 nor JpUHD/trCx43 cell lines showed any cAMP-mediated increase in the percentage of fused cells above control.

Fusion in the Full-Length Cx43 Lines Is Dependent on GJIC

As shown in Figure 2B, incubation of either the αhCG/Cx43 (48 h) or JpUHD/Cx43 (72 h) cell line with cAMP in the presence of the GJIC blocker CBX (white hatched bars) resulted in significant attenuation of the cAMP-mediated cell fusion ($P < 0.001$, n = 4, compared to cAMP alone). The inactive analog GZA had no effect on cAMP-stimulated cell fusion or in either cell line.

The GCM1 ERVW-1 Pathway Is Upstream of Cx43

Northern blot analysis of a 72-h time course of cAMP stimulation demonstrated a strong upregulation of *GCM1* mRNA levels by 24 h in wild-type Jeg3, αhCG/Cx43, JpUHD/Cx43, and JpUHD/trCx43 lines (Fig. 3A). The elevation in *GCM1* was sustained across the 48- and 72-h time points as compared to the respective controls at each time point. In contrast, *ERVW-1* mRNA levels were barely detectable at 24 h but increased by 48 and 72 h of cAMP stimulation (Fig. 3A). *GJA1* mRNA levels were also strongly induced by cAMP treatment in the αhCG/Cx43cell line and, to a lesser extent, in the JpUHD/Cx43 and JpUHD/trCx43 cell lines as compared to control time points (Supplemental Fig. S2). Northern blot analysis was unable to detect *GJA1* mRNA levels in the wild-type Jeg3 cell line under either control or cAMP conditions (Supplemental Fig. S2) [31]. To assess if GCM1 was acting to upregulate Cx43, the fusogenic BeWo choriocarcinoma cell was treated with forskolin (50 μM) in the presence of scrambled control siRNA (50 nM) or a cocktail of two *GCM1* siRNAs (50 nM). We have previously shown that this si*GCM1* treatment is effective in inhibiting the forskolin induction of *GCM1* in placental explants [21]. Real-time RT-PCR analysis of *GJA1* mRNA levels showed that forskolin induced a robust expression of *GJA1* in the presence of scrambled nonsilencing siRNA ($P < 0.01$, n = 4). In contrast, in the presence of *GCM1* siRNA, no forskolin-mediated increase in *GJA1* mRNA levels was detected (Fig. 3B). Similar results were seen when *GCM1* mRNA levels were assessed (Fig. 3B, inset).

Downregulation of SLC1A5 Only Occurs in Full-Length Cx43 Cell Lines

Real-time RT-PCR analysis of *SLC1A5* mRNA levels in the Jeg3, αhCG/Cx43, JpUHD/Cx43, and JpUHD/trCx43 cell lines demonstrated a time-dependent, significant decrease in *SLC1A5* in the cAMP-treated αhCG/Cx43 and JpUHD/Cx43 cell lines only (Fig. 4A). By 48 h of cAMP treatment, an 84.5% decrease in *SLC1A5* was observed in the αhCG/Cx43 cell line ($P < 0.01$, n =3) and a 60.34% decrease in the JpUHD/Cx43 line ($P < 0.01$, n = 3) as compared to the respective 48-h controls. A similar pattern of expression was observed at the protein level (Fig. 4, B and C). The SLC1A5 antibody detected a 70-kDa band in these cell lines, as observed in the representative photomicrograph (Fig. 4B). This observation corresponds to the molecular weight of SLC1A5 previously reported in brain extracts [32]. When SLC1A5 protein levels were expressed relative to those of the housekeeping protein α-TUBULIN, a significant 37.22% decrease in SLC1A5 levels was observed by 48 h of cAMP treatment ($P < 0.05$, n = 3) (Fig. 4C). Similarly, the JpUHD/Cx43 cell line showed a 74.16% decrease in SLC1A5 following cAMP treatment compared to the 48-h control samples ($P < 0.01$, n = 3). Neither the wild-type Jeg3 nor the JpUHD/trCx43 cell line showed any regulation of SLC1A5 at either the mRNA or protein level.

In Vitro Interaction of SLC1A5 and Cx43 in Cx43 Cell Lines and Villous Explants

Figure 5A presents a representative photomicrograph showing immunoprecipitation of SLC1A5 in the wild-type Jeg3, αhCG/Cx43, JpUHD/Cx43, and JpUHD/trCx43 cells followed by Western blot analysis for Cx43 (n = 3). The

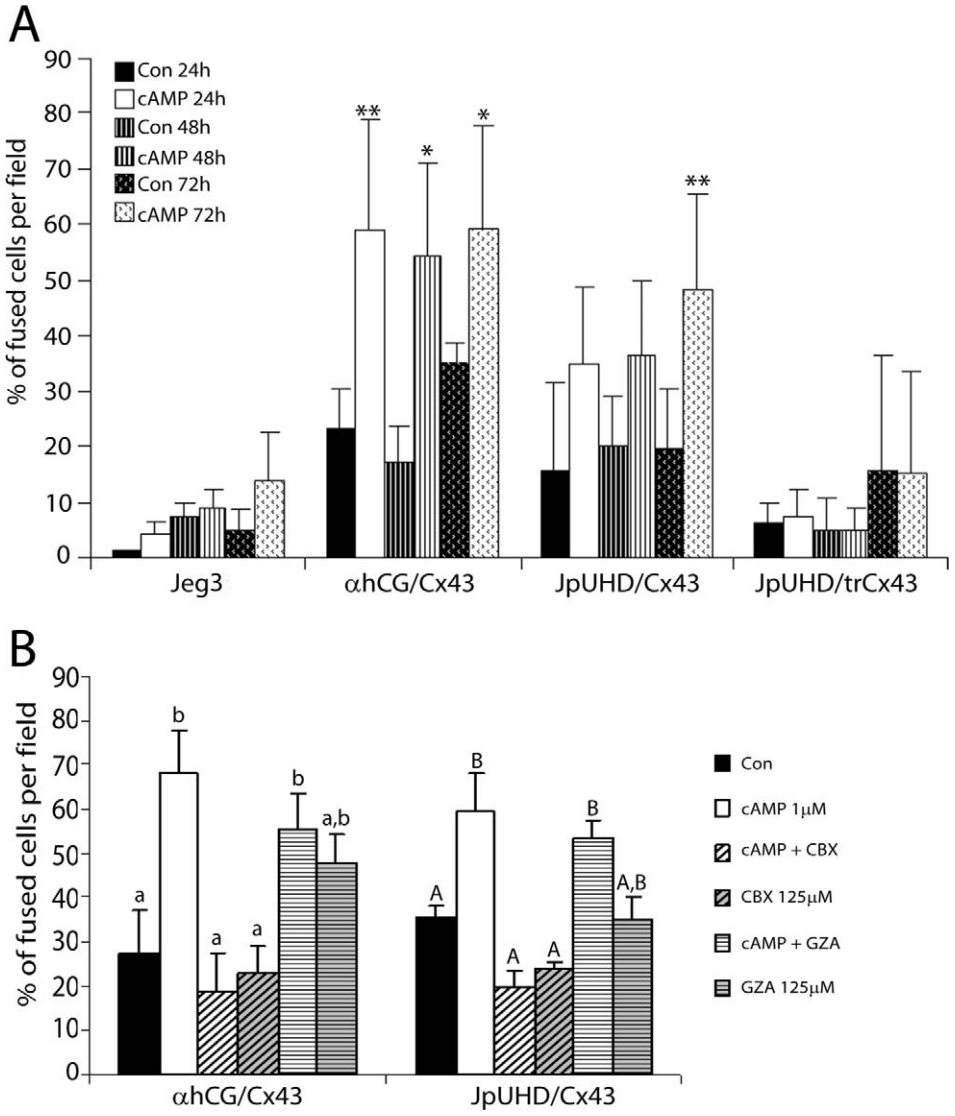

FIG. 2. Time-dependent increase in fusion is inhibited by blockade of GJIC or deletion of the cytoplasmic tail in the Cx43 cell lines. **A**) Quantification of the fusion events at 24 h (solid bars), 48 h (striped bars), and 72 h (spotted bars) in all cell lines under both control (black bars) and cAMP-treated conditions (white bars). The αhCG/Cx43 cell line demonstrated a high fusion rate, with more than 50% of the culture fused by 24 h on treatment with cAMP. This was maintained at both 48 and 72 h. The JpUHD/Cx43 line showed a slower rate of fusion, with only the 72-h cAMP-treated group showing a significant increase above control. Neither the Jeg3 nor JpUHD/trCx43 cells showed any increase in cell-cell fusion when stimulated with cAMP. $*P < 0.05$, $**P < 0.01$ in comparison to the respective control at each time point. **B**) Addition of the GJIC blocker 125 μM CBX to the αhCG/Cx43 (48 h) or JpUHD/Cx43 (72 h) cell line totally blocked the cAMP-stimulated cell fusion (white hatched bars compared to white, $P < 0.001$). The inactive CBX analog GZA (125 μM) had no effect on either cAMP-treated (white striped bars) or control conditions (gray striped bars). Different letters indicate significant differences ($P > 0.01$, $n = 4$).

monoclonal Cx43 antibody against the alpha1 domain of the Cx43 protein identified three bands characteristic of Cx43 (P0) and its phosphorylated forms (P1/P2) in the αhCG/Cx43, JpUHD/Cx43, and JpUDH/trCx43 cell lines under both control and cAMP-stimulated conditions. In the wild-type Jeg3 cells, a single weak band corresponding to nonphosphorylated Cx43 was observed under control conditions. Treatment with cAMP for 48 h increased the total P0 and P2 phosphorylated Cx43 band intensity in the wild-type Jeg3 and αhCG/Cx43 lines, whereas P0, P1, and P2 bands increased in the JpUHD/Cx43 line. In contrast, cAMP had little effect on the levels of either total or phosphorylated Cx43 in the JpUHD/trCx43 cell line ($n = 3$). A direct Western blot of Cx43 levels using a polyclonal Cx43 antibody in all cell lines showed that Jeg3 expressed a very low level of Cx43 protein under both control and cAMP conditions, whereas the Cx43-overexpressing lines had higher levels of Cx43, which increased on treatment with cAMP (Fig. 5B, $n = 3$). A cAMP-mediated increase in phosphorylated Cx43 was only observed in the αhCG/Cx43 cell line (Fig. 5B). The interaction of Cx43 and SLC1A5 was confirmed in both the αhCG/Cx43 cell line and first-trimester villous explants under control and cAMP-treated conditions by the reverse immunoprecipitation of Cx43 followed by Western blot analysis with a polyclonal goat anti-SLC1A5 antibody. A single 45-kDa band was observed, which increased in intensity in cAMP-treated villous explants (Fig. 5C, $n = 3$).

In Situ Colocalization of Cx43 and SLC1A5 in Fusing Cytotrophoblast

Triple immunofluorescent staining for SLC1A5 (red), E-cadherin (green), and Cx43 (blue) in a 7-wk, first-trimester

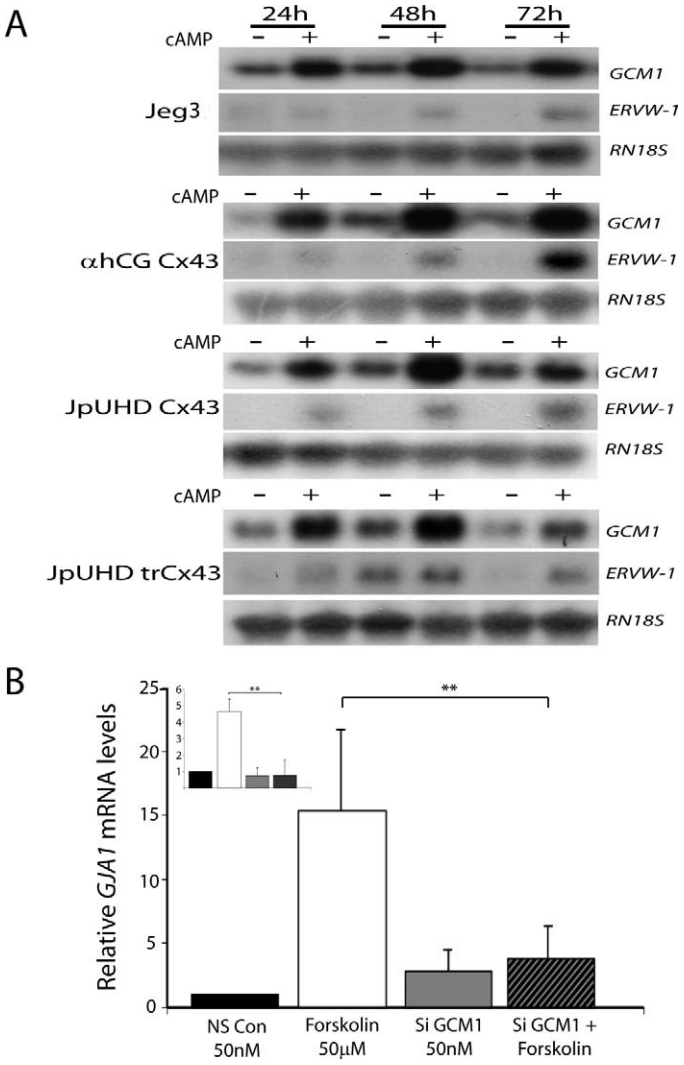

FIG. 3. **A**) Cyclic AMP stimulates GCM1 and ERVW-1 expression. Representative photomicrographs of Northern blot analysis of *GCM1, ERVW-1,* and *RN18S* mRNA levels following control (–) or 1 μM cAMP treatment (+) for 24, 48, and 72 h in wild-type Jeg3, αhCG/Cx43, JpUHD/Cx43, and JpUHD/trCx43 cell lines are shown. All probes detected a single band in each case: *GCM1*, 4 kb; *ERVW-1,* 3 kb; and *RN18S* rRNA, 2 kb. All cell lines showed a strong upregulation of *GCM1* by 24 h of cAMP stimulation; *ERVW-1* mRNA levels showed a slight increase at 24 h that was more strongly detected by 48 and 72 h of cAMP stimulation. **B**) GCM1 is upstream of Cx43. Real-time RT-PCR analysis of *GJA1* mRNA levels in BeWo choriocarcinoma cells demonstrated that stimulation with 50 μM forskolin in the presence of nonsilencing RNA resulted in the upregulation of *GJA1* mRNA levels. Silencing of *GCM1* (**inset**) resulted in the inhibition of forskolin-stimulated *GJA1* expression. Data are expressed relative to the level of *GJA1* mRNA in the control samples and standardized against the geometric mean of three housekeeping genes, *HPRT, YWHAZ,* and *RN18S* rRNA. $^{**}P < 0.01$, n = 4.

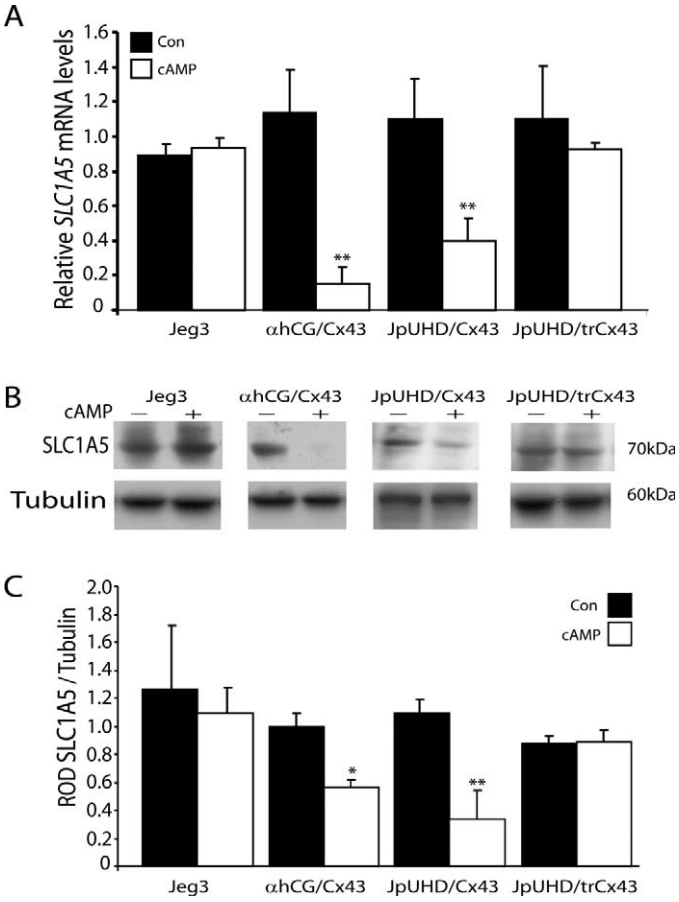

FIG. 4. Downregulation of SLC1A5 by cAMP in full-length Cx43-transfected cell lines. **A**) Real-time RT-PCR analysis of *SLC1A5* mRNA levels in wild-type Jeg3, αhCG/Cx43, JpUHD/Cx43, and JpUHD/trCx43 under control (black bars) and 1 μM cAMP treatment (white bars) for 48 h. Stimulation with 1 μM cAMP resulted in the significant decrease in *SLC1A5* mRNA levels in the αhCG/Cx43 and JpUHD/Cx43 cell lines only. Data are expressed relative to the level of *SLC1A5* mRNA in the control samples and standardized against the geometric mean of three housekeeping genes, *HPRT, YWHAZ,* and *18S* rRNA. **B**) Representative Western blot analysis demonstrating a single 70-kDa band corresponding to ASCT-2 protein. **C**) Stimulation with cAMP (+; white bars) over the 48-h time course resulted in the decrease in SLC1A5 levels in the αhCG/Cx43 and JpUHD/Cx43 cell lines when results were standardized against the housekeeping protein α-TUBULIN and expressed as the mean ± SD. $^{*}P < 0.05$, $^{**}P < 0.01$, n = 3.

placenta demonstrated that SLC1A5 was expressed across the syncytiotrophoblast and cytotrophoblast, whereas the cytotrophoblast was defined by strong E-cadherin expression in the plasma membrane (Fig. 6). At the site of fusion of a daughter cytotrophoblast with the overlying syncytium, E-cadherin staining was lost, and an increased density of Cx43 gap junction plaques was observed colocalizing with SLC1A5 (Fig. 6A, arrows). In a quiescent area of the same placenta where no cytotrophoblast fusion was observed and E-cadherin marked a complete layer of underlying cytotrophoblast, low levels of Cx43 were detected in the cytotrophoblast membranes (Fig. 6B). No staining was observed in the goat IgG control (Fig. 6C) or the dual mouse-rabbit IgG control (Fig. 6D).

DISCUSSION

In the present study, we demonstrate that the full-length Cx43 protein is required for cAMP-stimulated trophoblast cell-cell fusion. Moreover, the GJIC blocker CBX inhibits the cAMP-mediated fusion in the full-length Cx43 cell lines, suggesting dependency on Cx43-mediated GJIC. Although CBX can also inhibit cell-cell communication via pannexins, our data support the observations initially made by Cronier et al. [4], in which heptanol-mediated blockade of GJIC inhibited primary cytotrophoblast cell fusion. This GJIC was subsequently shown to be mediated by Cx43 [5] and regulated by hCG [3], whereas administration of Cx43 antisense oligonucleotides prevented primary cytotrophoblast fusion [33]. However, the present study adds further evidence to support a pivotal role for the Cx43 cytoplasmic tail in the regulation of

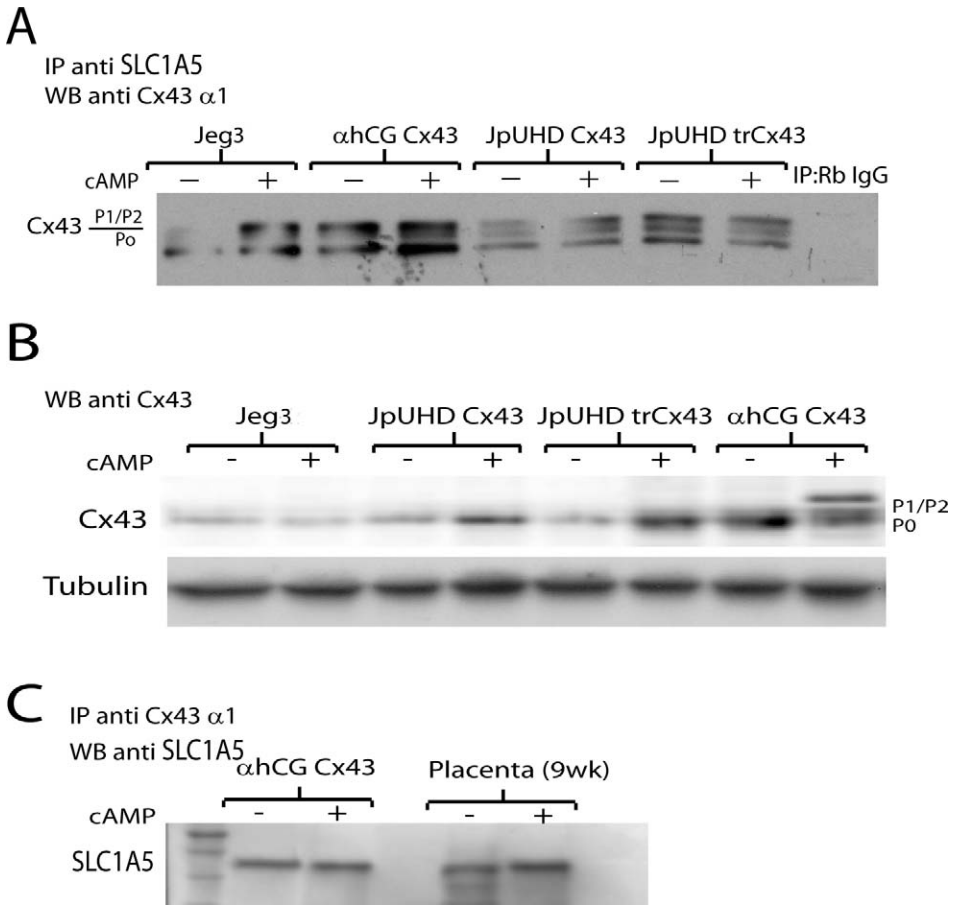

FIG. 5. Interaction of SLC1A5 and Cx43 in vitro. **A**) Representative Western blot of Cx43 levels in SLC1A5 immunoprecipitates from wild-type Jeg3, αhCG/Cx43 JpUHD/Cx43, and JpUHD/trCx43 cell lines stimulated with control (–) or 1 μM cAMP (+) for 48 h. The monoclonal Cx43 antibody against the alpha domain of Cx43 recognized a specific 43-kDa band and two higher bands corresponding to phosphorylated Cx43. The nonspecific rabbit IgG control for the immunoprecipitation showed no band (n = 3). **B**) Representative Western blot of Cx43 levels in wild-type Jeg3, αhCG/Cx43 JpUHD/Cx43, and JpUHD/trCx43 cell lines stimulated with control (–) or 1 μM cAMP (+) for 48 h**.** The polyclonal Cx43 antibody recognized a 43-kDa band that was detected at very low levels in the wild-type Jeg3 and increased on cAMP treatment in the Cx43 cell lines as compared to the housekeeping protein α-TUBULIN. **C**) Representative Western blot of SLC1A5 in Cx43 immunoprecipitates from αhCG/Cx43 cells and placental villous explants stimulated with control (–) or 1 μM cAMP (+) for 48 or 24 h, respectively**.** The polyclonal goat anti-SLC1A5 antibody detected a 45-kDa band in all samples, which increased in intensity in cAMP-treated explants as compared to controls (n = 3).

trophoblast cell fusion. The trCx43 protein, which is a functional gap junction channel (although improperly gated) that mediates cell-cell coupling and Lucifer yellow as well as calcein dye transfer [13, 34, 35], did not enable cAMP-mediated fusion in our experiments. These results suggest that both GJIC and intracellular signaling via the carboxyterminus of Cx43 play important roles in trophoblast cell fusion.

Interestingly, in our experiments, the constitutively expressing Cx43 line αhCG/Cx43 showed the most sensitivity to 8-bromo-cAMP and the largest increase in the percentage of fused cells. This can be explained by the fact that cAMP can upregulate αhCG via its promoter [36] and, therefore, also drives Cx43 expression in this cell line. Northern blot analysis showed a high level of Cx43 mRNA in the cAMP-treated samples over a 72-h time course (Supplemental Fig. S2). The high expression level of Cx43 would thus result in increased GJIC and efficient cell-cell fusion, as observed across the entire culture by the extensive comixing of the green and red cytoplasmic dyes. The two-color fusion assay has previously been shown to be a robust and accurate method to quantify syncytial formation [26]. Indeed, as those authors stated, this is the only method able to discriminate whether a multinucleated cell body arises from cell-cell fusion or from endomitosis, as seen in our overexpressing Cx40 cell line (Supplemental Fig. S1).

We further show that cAMP stimulation upregulates the transcription factor GCM1 and its downstream effector ERVW-1 in all of the Cx43-transfected and wild-type Jeg3 cell lines. The effects of cAMP on GCM1 and ERVW-1 are mediated by the cAMP-dependent protein kinase A (PKA) signaling pathway [37]. In primary trophoblast and BeWo choriocarcinoma cells, cAMP is thought to contribute to increased GCM1 expression via cAMP-responsive element modulator (CREM) or cAMP-responsive element-binding (CREB) transcription factor binding in the *GCM1* promoter and to increased GCM1 protein stability [37]. We have shown that GCM1 acts as a molecular switch in the human placenta, where it governs the differentiation of the cytotrophoblast from a proliferating phenotype to the G_0 cytotrophoblast cell that fuses with the syncytiotrophoblast [20, 21]. Silencing of *GCM1* leads to accelerated cytotrophoblast proliferation, whereas forskolin induction of syncytialization leads to increased *GCM1* mRNA levels [21]. *ERVW-1* mRNA levels are also known to increase with the differentiation and fusion of cytotrophoblast [38]. However, our present data demonstrate that this cAMP-stimulated expression of *GCM1* and *ERVW-1*

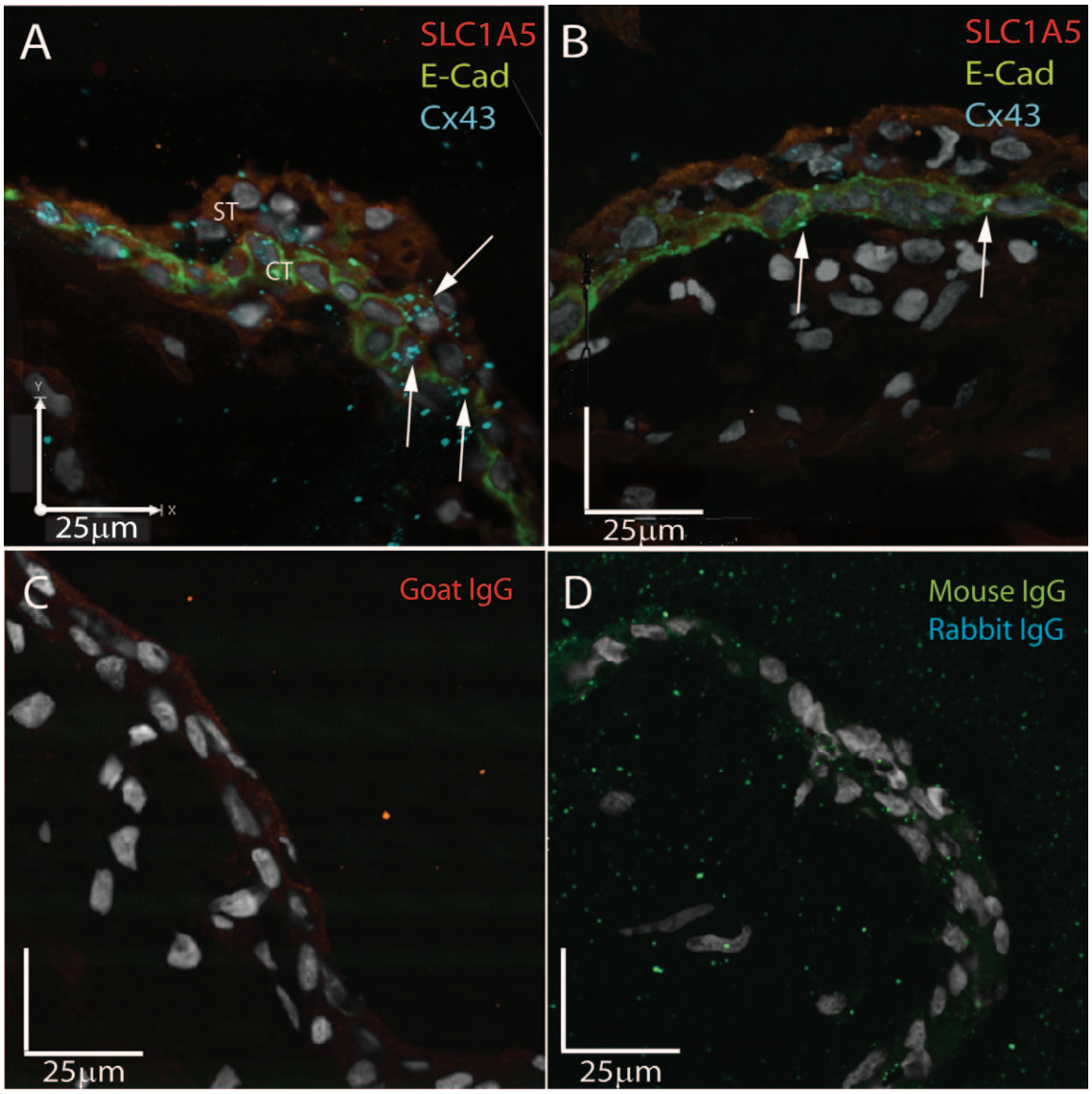

FIG. 6. Fusing cytotrophoblast demonstrates in situ colocalization of Cx43 and SLC1A5. Representative triple immunofluorescent images of SLC1A5 (red), E-cadherin (green), and Cx43 (blue) expression in first-trimester placental sections are shown. **A**) In areas of cell fusion shown by loss of E-cadherin, Cx43 and SLC1A5 colocalize (arrows) to the junction of the apical membrane of the cytotrophoblast and the basal membrane of the syncytiotrophoblast. **B**) In quiescent areas of the same placenta, no colocalization is observed, and Cx43 is restricted to the cytotrophoblast cell junctions. **C**) Nonspecific goat IgG control. **D**) Nonspecific dual IgG controls of mouse and rabbit IgGs. Bar = 25 μM.

mRNA is not affected by expression of the different Cx43 constructs and occurs in both the fusing and nonfusing cell lines. Thus, activation of this pathway may not be sufficient for cell fusion. Moreover, we have shown that silencing of *GCM1* in the naturally fusogenic cell line BeWo results in the inhibition of forskolin-induced *GJA1* mRNA expression. Therefore, we conclude that GCM1 expression and function is upstream of Cx43, but also that fully functional Cx43 GJIC is essential for subsequent cell-cell fusion.

We also demonstrate that the cAMP-mediated fusion observed in the full-length Cx43 lines correlates with the downregulation of SLC1A5 at both the mRNA and protein levels. This decrease in SLC1A5 levels was not observed in either the nonfusing wild-type Jeg3 or JpUHD/trCx43 cell lines. These results are similar to those reported by Kudo and Boyd [39], who demonstrated decreased *SLC1A5* mRNA levels together with a concomitant decrease in amino acid transport mediated by the ATB(0) transporter activity in forskolin-stimulated BeWo cells. It is possible that SLC1A5 is downregulated as a consequence of cell fusion rather than preceding or even promoting fusion. Further experiments would shed light on this matter. In the present study, triple immunohistochemical analysis demonstrated that SLC1A5 was expressed throughout the syncytiotrophoblast and cytotrophoblast and colocalized with an increased level of Cx43 gap junctions in the junction of the apical cytotrophoblast and basal syncytiotrophoblast membrane at sites of active cytotrophoblast cell fusion in first-trimester placenta. Cytotrophoblast fusion was identified by the by loss of E-cadherin staining of the apical cytotrophoblast membrane in fusing cells. The syncytial expression pattern of SLC1A5 correlates well with the reported localization of the neutral amino acid transporter system in the human placenta [39–41]. We also observed SLC1A5 expression at a low level in the cytotrophoblast, similar to reports by Hayward et al. [42]. Those authors were surprised by the lack of SLC1A5 in the syncytiotrophoblast

membrane, and we suggest that these differences may be explained by the different antibodies used. In the present study, the commercially available anti-SLC1A5 antibody used detected a major 70-kDa band in the Cx43 cell line lysates by Western blot analysis, whereas the study by Hayward et al. used a rabbit antisera that detected two 45- and 53-kDa bands. We also show that in quiescent areas of the same first-trimester placenta, identified by a complete cytotrophoblast layer marked by E-cadherin staining, low levels of Cx43 gap junctions were restricted to the cytotrophoblast layer. This staining was shown to be specific by the use of nonimmune rabbit, mouse, and goat IgGs.

The colocalization of Cx43 and SLC1A5 was further demonstrated by immunoprecipitation of SLC1A5 followed by Western blot analysis with anti-Cx43 antibody. Interestingly, cAMP mediated an increase in associated Cx43 P2 band in the wild-type Jeg3 and P1 and P2 bands in the full-length Cx43 cell lines only. This is unsurprising, because the P1-P2 shift is induced by the phosphorylation of numerous serine residues within the carboxyterminal tail of Cx43 [43, 44], which are missing in the JpUHD/trCx43 cell line. A direct Western blot of Cx43 levels showed that Jeg3 cells express a low level of Cx43 and that cAMP has no effect on upregulation of Cx43 levels (mRNA levels were undetectable by Northern blot analysis) (Supplemental Fig. S2A). Thus, we suggest that the levels of Cx43 in the wild-type Jeg3 are insufficient to contribute to enough Cx43 gap junctions to initiate cell-cell fusion. In contrast, in the overexpressing Cx43 cell lines, Cx43 mRNA and protein levels were upregulated by cAMP, and phosphorylation was increased in the αhCG/Cx43 cell line. Similar to the regulation of GCM1 and ERVW-1, the cAMP-mediated increase in Cx43 phosphorylation is also mediated by the PKA pathway and leads to increased Cx43 protein within gap junction plaques in the plasma membrane [45, 46]. In particular, the P2 isoform, which increased in association with SLC1A5 in the present study, is associated with the G_0/G_1 phase of the cell cycle and with the scaffolding proteins TJP1 and TJP2 at the plasma membrane [47]. Thus, the immunoprecipitation data support our finding of increased Cx43 gap junctions associated with SLC1A5 in areas of cytotrophoblast fusion. This interaction was confirmed by the reverse immunoprecipitation of Cx43 followed by Western blot analysis with SLC1A5 in both the αhCG/Cx43 cell line and first-trimester placental villous explants. Interestingly, the level of SLC1A5 bound to Cx43 was high in the control explants, demonstrating in vivo interaction and correlating with the high degree of fusion during this period of gestation, but it also increased when treated with cAMP. We have previously shown that cAMP treatment of placental explants depletes the cytotrophoblast population and accelerates fusion into the syncytiotrophoblast [21], thus correlating with an increased association of SLC1A5 with Cx43 gap junctions.

Importantly, the TJP1 protein has also been demonstrated to be functionally required for trophoblast cell fusion [17] and to interact with the last 20 amino acids on the carboxyterminal tail of Cx43 [16]. Silencing of TJP1 prevented primary term trophoblast fusion and resulted in a decrease in Cx43 protein expression, which was suggested to be due to the destabilization of a supramolecular complex [17]. Our data demonstrating the lack of fusion in the JpUHD/trCx43 cell line further supports the critical role of this tight junction-gap junction interaction in the stimulation of trophoblast fusion. Moreover, we suggest that SLC1A5 may be another putative member of this fusion supramolecule, yet its interaction with CX43 is not mediated via the C-terminus but, rather, through the interaction of the transmembrane domains of SLC1A5 and Cx43 in the plasma membrane. It is possible that the formation of Cx43 gap junctions spanning the cytotrophoblast apical membrane and syncytiotrophoblast basal membrane preferentially sequester SLC1A5 to the basal syncytiotrophoblast membrane and the site of its interaction with ERVW-1.

In conclusion, our data support and extend the ERVW-1-SLC1A5 interaction model of trophoblast cell fusion proposed by Potgens et al. [25]. In this model, SLC1A5 is in excess to ERVW-1 in the syncytiotrophoblast basal membrane until activation of cell fusion when SLC1A5 decreases [25]. Our data suggest the following modifications to this model: In nonfusing regions of the placenta, SLC1A5 is in excess of ERVW-1 until activation of PKA signaling in a differentiating cytotrophoblast increases GCM1 and ERVW-1 and may decrease SLC1A5. The PKA signaling also phosphorylates Cx43, which induces gap junction plaque formation between cytotrophoblast and syncytiotrophoblast and the association of TJP1 with the cytoplasmic domain of Cx43. The interaction of Cx43 and SLC1A5 in the syncytiotrophoblast basal membrane subsequently brings SLC1A5 into proximity with ERVW-1 and stimulates cytotrophoblast fusion with the syncytium. Our data demonstrate a critical, central role for Cx43 in mediating both GJIC and protein-protein interaction with SLC1A5 to stimulate trophoblast cell fusion.

ACKNOWLEDGMENT

The authors thank Ms. Sabrina Pavri and Ms. Iskra Peltekova for their work on the two-color fusion assay and quantification of the fusion indices during their summer student projects. The authors also thank the donors, the Research Centre for Women's and Infants' Health BioBank Program of the Canadian Institutes of Health Research (CIHR) Group in Development and Fetal Health (CIHR MGC-13299), the Samuel Lunenfeld Research Institute, and the Mount Sinai Hospital/University Health Network Department of Obstetrics and Gynecology for the human specimens used in the present study.

REFERENCES

1. Benirschke K, Kaufman P, Baergen R. Pathology of the Human Placenta. New York: Springer; 2006.
2. Kingdom J, Huppertz B, Seaward G, Kaufmann P. Development of the placental villous tree and its consequences for fetal growth. Eur J Obstet Gynecol Reprod Biol 2000; 92:35–43.
3. Cronier L, Herve JC, Deleze J, Malassine A. Regulation of gap junctional communication during human trophoblast differentiation. Microsc Res Tech 1997; 38:21–28.
4. Cronier L, Frendo JL, Defamie N, Pidoux G, Bertin G, Guibourdenche J, Pointis G, Malassine A. Requirement of gap junctional intercellular communication for human villous trophoblast differentiation. Biol Reprod 2003; 69:1472–1480.
5. Cronier L, Defamie N, Dupays L, Theveniau-Ruissy M, Goffin F, Pointis G, Malassine A. Connexin expression and gap junctional intercellular communication in human first trimester trophoblast. Mol Hum Reprod 2002; 8:1005–1013.
6. Kardami E, Dang X, Iacobas DA, Nickel BE, Jeyaraman M, Srisakuldee W, Makazan J, Tanguy S, Spray DC. The role of connexins in controlling cell growth and gene expression. Prog Biophys Mol Biol 2007; 94: 245–264.
7. Vinken M, Vanhaecke T, Papeleu P, Snykers S, Henkens T, Rogiers V. Connexins and their channels in cell growth and cell death. Cell Signal 2006; 18:592–600.
8. Huppertz B, Bartz C, Kokozidou M. Trophoblast fusion: fusogenic proteins, SYNCYTINs and ADAMs, and other prerequisites for syncytial fusion. Micron 2006; 37:509–517.
9. Omori Y, Yamasaki H. Mutated connexin43 proteins inhibit rat glioma cell growth suppression mediated by wild-type connexin43 in a dominant-negative manner. Int J Cancer 1998; 78:446–453.
10. Xu X, Li WE, Huang GY, Meyer R, Chen T, Luo Y, Thomas MP, Radice GL, Lo CW. Modulation of mouse neural crest cell motility by N-cadherin and connexin 43 gap junctions. J Cell Biol 2001; 154:217–230.
11. Lin JH, Takano T, Cotrina ML, Arcuino G, Kang J, Liu S, Gao Q, Jiang L, Li F, Lichtenberg-Frate H, Haubrich S, Willecke K, et al. Connexin 43

enhances the adhesivity and mediates the invasion of malignant glioma cells. J Neurosci 2002; 22:4302–4311.
12. Olbina G, Eckhart W. Mutations in the second extracellular region of connexin 43 prevent localization to the plasma membrane, but do not affect its ability to suppress cell growth. Mol Cancer Res 2003; 1: 690–700.
13. Gellhaus A, Dong X, Propson S, Maass K, Klein-Hitpass L, Kibschull M, Traub O, Willecke K, Perbal B, Lye SJ, Winterhager E. Connexin 43 interacts with NOV: a possible mechanism for negative regulation of cell growth in choriocarcinoma cells. J Biol Chem 2004; 279:36931–36942.
14. Gellhaus A, Schmidt M, Dunk C, Lye SJ, Kimmig R, Winterhager E. Decreased expression of the angiogenic regulators CYR61 (CCN1) and NOV (CCN3) in human placenta is associated with pre-eclampsia. Mol Hum Reprod 2006; 12:389–399.
15. Lampe PD, Lau AF. Regulation of gap junctions by phosphorylation of connexins. Arch Biochem Biophys 2000; 384:205–215.
16. Toyofuku T, Yabuki M, Otsu K, Kuzuya T, Hori M, Tada M. Direct association of the gap junction protein connexin-43 with ZO-1 in cardiac myocytes. J Biol Chem 1998; 273:12725–12731.
17. Pidoux G, Gerbaud P, Gnidehou S, Grynberg M, Geneau G, Guibourdenche J, Carette D, Cronier L, Evain-Brion D, Malassine A, Frendo JL. ZO-1 is involved in trophoblastic cell differentiation in human placenta. Am J Physiol Cell Physiol 2010; 298:C1517–C1526.
18. Huppertz B, Kingdom JC. Apoptosis in the trophoblast—role of apoptosis in placental morphogenesis. J Soc Gynecol Investig 2004; 11:353–362.
19. Huppertz B, Kaufmann P, Kingdom J. Trophoblast turnover in health and disease. Fetal Matern Med Rev 2002; 13:103–118.
20. Baczyk D, Satkunaratnam A, Nait-Oumesmar B, Huppertz B, Cross JC, Kingdom JC. Complex patterns of GCM1 mRNA and protein in villous and extravillous trophoblast cells of the human placenta. Placenta 2004; 25:553–559.
21. Baczyk D, Drewlo S, Proctor L, Dunk C, Lye S, Kingdom J. Glial cell missing-1 transcription factor is required for the differentiation of the human trophoblast. Cell Death Differ 2009; 16:719–727.
22. Blond JL, Lavillette D, Cheynet V, Bouton O, Oriol G, Chapel-Fernandes S, Mandrand B, Mallet F, Cosset FL. An envelope glycoprotein of the human endogenous retrovirus HERV-W is expressed in the human placenta and fuses cells expressing the type D mammalian retrovirus receptor. J Virol 2000; 74:3321–3329.
23. Lin C, Lin M, Chen H. Biochemical characterization of the human placental transcription factor GCMa/1. Biochem Cell Biol 2005; 83: 188–195.
24. Lavillette D, Marin M, Ruggieri A, Mallet F, Cosset FL, Kabat D. The envelope glycoprotein of human endogenous retrovirus type W uses a divergent family of amino acid transporters/cell surface receptors. J Virol 2002; 76:6442–6452.
25. Potgens AJ, Drewlo S, Kokozidou M, Kaufmann P. SYNCYTIN: the major regulator of trophoblast fusion? Recent developments and hypotheses on its action. Hum Reprod Update 2004; 10:487–496.
26. Borges M, Bose P, Frank HG, Kaufmann P, Potgens AJ. A two-color fluorescence assay for the measurement of syncytial fusion between trophoblast-derived cell lines. Placenta 2003; 24:959–964.
27. Mitchell JA, Ting TC, Wong S, Mitchell BF, Lye SJ. Parathyroid hormone-related protein treatment of pregnant rats delays the increase in connexin 43 and oxytocin receptor expression in the myometrium. Biol Reprod 2003; 69:556–562.
28. Shynlova O, Mitchell JA, Tsampalieros A, Langille BL, Lye SJ. Progesterone and gravidity differentially regulate expression of extracellular matrix components in the pregnant rat myometrium. Biol Reprod 2004; 70:986–992.
29. Chen CP, Wang KG, Chen CY, Yu C, Chuang HC, Chen H. Altered placental SYNCYTIN and its receptor ASCT2 expression in placental development and pre-eclampsia. BJOG 2006; 113:152–158.
30. Baczyk D, Dunk C, Huppertz B, Maxwell C, Reister F, Giannoulias D, Kingdom JC. Bipotential behavior of cytotrophoblasts in first trimester chorionic villi. Placenta 2006; 27:367–374.
31. Hellmann P, Grummer R, Schirrmacher K, Rook M, Traub O, Winterhager E. Transfection with different connexin genes alters growth and differentiation of human choriocarcinoma cells. Exp Cell Res 1999; 246:480–490.
32. Lim J, Lorentzen KA, Kistler J, Donaldson PJ. Molecular identification and characterization of the glycine transporter (GLYT1) and the glutamine/glutamate transporter (ASCT2) in the rat lens. Exp Eye Res 2006; 83:447–455.
33. Frendo JL, Cronier L, Bertin G, Guibourdenche J, Vidaud M, Evain-Brion D, Malassine A. Involvement of connexin 43 in human trophoblast cell fusion and differentiation. J Cell Sci 2003; 116:3413–3421.
34. Fishman GI, Moreno AP, Spray DC, Leinwand LA. Functional analysis of human cardiac gap junction channel mutants. Proc Natl Acad Sci U S A 1991; 88:3525–3529.
35. Maass K, Ghanem A, Kim JS, Saathoff M, Urschel S, Kirfel G, Grummer R, Kretz M, Lewalter T, Tiemann K, Winterhager E, Herzog V, et al. Defective epidermal barrier in neonatal mice lacking the C-terminal region of connexin43. Mol Biol Cell 2004; 15:4597–4608.
36. Jameson JL, Powers AC, Gallagher GD, Habener JF. Enhancer and promoter element interactions dictate cyclic adenosine monophosphate mediated and cell-specific expression of the glycoprotein hormone alpha-gene. Mol Endocrinol 1989; 3:763–772.
37. Knerr I, Schubert SW, Wich C, Amann K, Aigner T, Vogler T, Jung R, Dotsch J, Rascher W, Hashemolhosseini S. Stimulation of GCMa and SYNCYTIN via cAMP-mediated PKA signaling in human trophoblastic cells under normoxic and hypoxic conditions. FEBS Lett 2005; 579: 3991–3998.
38. Frendo JL, Olivier D, Cheynet V, Blond JL, Bouton O, Vidaud M, Rabreau M, Evain-Brion D, Mallet F. Direct involvement of HERV-W Env glycoprotein in human trophoblast cell fusion and differentiation. Mol Cell Biol 2003; 23:3566–3574.
39. Kudo Y, Boyd CA. Changes in expression and function of SYNCYTIN and its receptor, amino acid transport system B(0) (ASCT2), in human placental choriocarcinoma BeWo cells during syncytialization. Placenta 2002; 23:536–541.
40. Johnson LW, Smith CH. Neutral amino acid transport systems of microvillous membrane of human placenta. Am J Physiol Cell Physiol 1988; 254:C773–C780.
41. Hoeltzli SD, Smith CH. Alanine transport systems in isolated basal plasma membrane of human placenta. Am J Physiol Cell Physiol 1989; 256: C630–C637.
42. Hayward MD, Potgens AJ, Drewlo S, Kaufmann P, Rasko JE. Distribution of human endogenous retrovirus type W receptor in normal human villous placenta. Pathology 2007; 39:406–412.
43. Solan JL, Lampe PD. Key connexin 43 phosphorylation events regulate the gap junction life cycle. J Membr Biol 2007; 217:35–41.
44. Lampe PD, Cooper CD, King TJ, Burt JM. Analysis of connexin 43 phosphorylated at S325, S328 and S330 in normoxic and ischemic heart. J Cell Sci 2006; 119:3435–3442.
45. Burghardt RC, Barhoumi R, Sewall TC, Bowen JA. Cyclic AMP induces rapid increases in gap junction permeability and changes in the cellular distribution of connexin43. J Membr Biol 1995; 148:243–253.
46. Yogo K, Ogawa T, Akiyama M, Ishida-Kitagawa N, Sasada H, Sato E, Takeya T. PKA implicated in the phosphorylation of CX43 induced by stimulation with FSH in rat granulosa cells. J Reprod Dev 2006; 52: 321–328.
47. Singh D, Solan JL, Taffet SM, Javier R, Lampe PD. Connexin 43 interacts with zona occludens-1 and -2 proteins in a cell cycle stage-specific manner. J Biol Chem 2005; 280:30416–30421.